Nonlinear Compensation of Two-Dimensional Contouring Servomechanism

SAWARAGI, Yoshikazu; AKASHI, Hajime; TERAISHI, Minoru; FUKUDA, Takehito

Nonlinear Compensation of Two-Dimensional Contouring Servomechanism

By

Yoshikazu SAWARAGI*, Hajime AKASHI**, Minoru TERAISHI*
and Takehito FUKUDA*

(Received June 30, 1966)

This paper gives a method of nonlinear compensation for a two-dimensional contouring servomechanism, by which the cornering error, or the transient error at the corner of a figure being traced, is held within given tolerance.

The effect of compensation is analyzed by graphical means, using the result of model experiment and the parameters are determined so as to obtain the desirable performance.

Stability analysis of the system is also given utilizing the describing function method. The result is applied to an actual automatic flame cutting machine and the practicability is proved.

1. Introduction

Various attempts have been made by many authors to study the effect of inserting nonlinear elements to compensate the effects of other inherent nonlinearities, or to obtain a better performance than would be achieved utilizing linear elements[1]. In view of application, it is particularly interesting to investigate the way of compensating backlash, because it is a common nonlinearity in many servomechanisms.

For example, C.N. Shen intentionally incorporated a second nonlinearity, a dead zone, in the input to the integrator in order to stabilize a second-order servomechanism with backlash for small signals[2]. Unfortunately, however, this dead zone introduces offset, and so another nonlinearity, a saturable velocity feedback, was also incorporated in the error signal. In this way, he succeeded in stabilizing the system under step input as well as eliminating excessive error under ramp input[3]. A.K. Mahalanabis also investigated the effects of coulomb friction in feedback systems having backlash and revealed that this friction has beneficial effects on stability[4]. On the other hand, C.N. Shen & H. Wang dealt with dry friction and used a dead zone before the integrator to decrease

* Department of Applied Mathematics and Physics.
** Department of Mechanical Engineering, Doshisha University.

the steady--state error at high ramp rates and to achieve stability[5].

In the above-mentioned studies, the authors aim primarily at stabilizing systems by introducing intentionally nonlinear compensation. The problem that we are concerned with, however, is the achievement of the best performance in both the transient and equilibrium state. In view of this fact, we have devoted ourselves to the improvement of the transient response of a nonlinear servomechanism having three inherent nonlinearities.

The practical problem treated in this paper is to examine the transient error at a corner formed by two perpendicularly intersecting straight lines of a two-dimensional nonlinear contouring servomechanism consisting of two one-dimensional servomechanisms with identical characteristics.

We will first define the overshooting error following a ramp input and then propose a nonlinear compensation such that the overshooting errors for various ramp rates are held within a given tolerable value. Since entirely analytical investigation of the effect of compensation is difficult, we chose a comparatively simple method of determining an optimal nonlinearity based upon experimental results using a model and the inverse describing function.

2. Overshooting Error

With respect to the two-dimensional contouring servomechanism, F.J. Ellert[6], H.E. Vigour[7], and others have made interesting studies. With their results in mind, we will discuss the problems encountered in the design of a two-dimensional servomechanism.

Here we treat the case in which a prescribed figure is traced by a two-dimensional nonlinear contouring servomechanism, which, as its name implies, consists of two nonlinear servomechanisms positioned along two mutually perpendicular machine axes which we shall call X-and Y-axis.

In practice, two-dimensional contouring systems are used to move a tool, such as milling cutter, lathe tool, drafting pen, or the burner of an automatic flame cutting machine.

Now, to make the problem tractable, it is assumed that the two servomechanisms treated are identical, because they are mostly of the same general type in practical cases and can reasonably be assumed to be so if they are not. The block diagram of the system is given in Fig. 1.

Of various possible figures to be traced which may consist of straight lines, circular arcs, and other curves, we treat here the portion composed of two straight line segments intersecting at an angle as shown in Fig. 2. The choice is due to

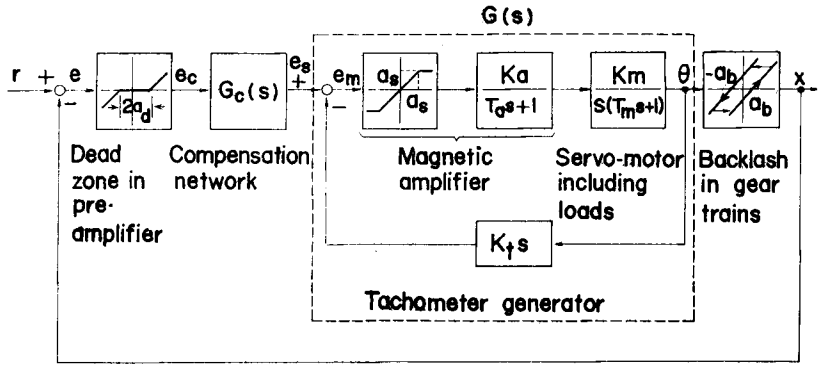

Fig. 1. Block diagram of the nonlinear servomechanism.

practical reasons that the curved figures may often be broken up into a series of straight lines and machine parts often have corners. In this figure, B represents a corner, the line segment AB runs parallel to the X-axis and the line segment BC cuts the X-axis at an angle Φ.

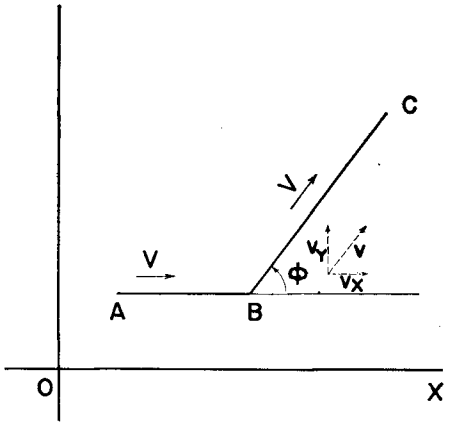

Fig. 2. A corner.

When a curve ABC is traced by a two-dimensional contouring system with a constant feed rate, there will be overshoot or undershoot errors at the corner. To decrease such errors, we should decrease the error of the servomechanism along X- and Y-axis, since the two servomechanisms are mechanically independent.

Suppose that such an apparatus moves at an angle Φ with the direction of the X-axis. Let the feed rate be V, then the feed rate components of the X-axis and Y-axis, V_X and V_Y, are given by

$$V_X = V\cos\Phi\,, \quad V_Y = V\sin\Phi\,. \tag{1}$$

Thus when the apparatus tracks ABC, it moves first on the line AB with the feed rate components $V_X=V$ and $V_Y=0$, and then the feed rate components change to $V_X=V\cos\Phi$, and $V_Y=V\sin\Phi$. On the line BC, the same feed rate will be maintained.

Generally speaking, the overshoot will be in proportion to the derivative of the feed rate. Since the derivative of V at a corner has the maximum value when $\Phi=90°$ $(0<\Phi\leqslant 90°)$, the value of the overshoot will be the maximum when the

corner is right-angled. The definition of the overshooting error E_0 and undershooting error E_u are given in Fig. 3 (a) and Fig. 3 (b).

The typical transient response to a ramp rate input is shown in Fig. 4. The

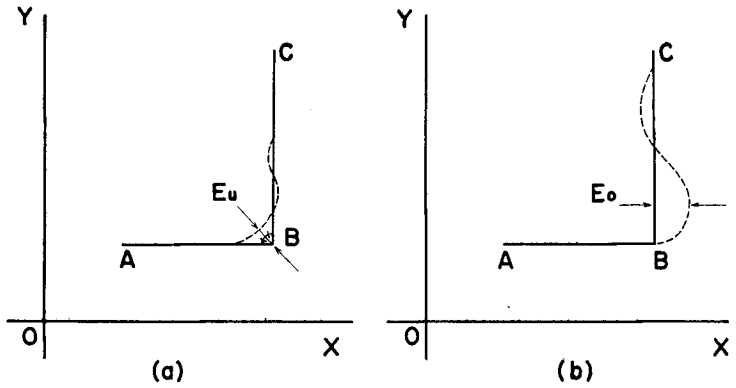

Fig. 3. (a) Undershooting error. (b) Overshooting error.

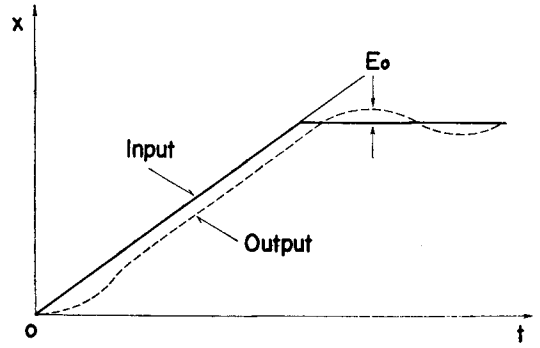

Fig. 4. Typical overshooting error E_0 following a ramp input.

overshooting error E_0 here is evidently equal to the overshooting error in Fig. 3 (a). The maximum overshooting error for varied ramp inputs is denoted by $E_{0\max}$.

The problem may now be stated as follows: In order to decrease the overshooting error E_0 so that it is within a given tolerance for any ramp input, find an appropriate compensation network for this servomechanism.

3. Linear Compensation Device

In this section we will describe how the overshooting error may be reduced to some extent by introducing a conventional linear compensation involving *CR*-lead network in cascade to the system. The result, however, can never meet our require-

ments. Therefore, we devote the next section to the analysis of the case where an intentionally nonlinear element is employed to obtain satisfactory results.

Since the servomechanism treated here involves essentially three types of nonlinearities, a dead zone in the pre-amplifier, saturation in the magnetic amplifier, and backlash in gear trains, it is difficult to examine entirely analytically the effects of compensation devices.

In this study, therefore, they are examined by experiments of a model and an analog computer.

3.1. Proportional plus derivative compensation device

First, we employed a series compensation, proportional plus derivative element $1+\kappa s$. The compensation device is represented by the transfer function $G_c(s)$ in Fig. 1. The result of the experiments using an analog computer shows that, for the constant ramp rate, the overshooting error E_0 decreases as the value of κ is increased.

The same result was obtained by the experiments using a model. The overshooting error, however, may be decreased only to a certain extent by increasing the value of κ, because the system becomes unstable or oscillatory when κ is made excessively large.

It becomes necessary, therefore, to introduce still another component. If the forward phase shift is introduced at the frequency where the system would oscillate, the stability of the system would be guaranteed. Hence the *CR*-phase lead network was introduced in cascade with the derivative element κs.

3.2. Insertion of the *CR*-phase lead network

In place of the above-mentioned compensation, however, we actually used another compensation including *CR*-phase lead network as shown in Fig. 5. As the result of similar experiments, we could determine the value of a and T of the *CR*-phase lead network such that the phase shift is positive at the frequency where the system would oscillate, and select the optimal value of κ such that the overshooting error E_0 is zero for a certain ramp rate r_0. For ramp rates over r_0, we had an overshoot and for ramp rates less than r_0 we had an undershoot. The stability of the system was assured. Experimental results using a model are shown in Fig. 6.

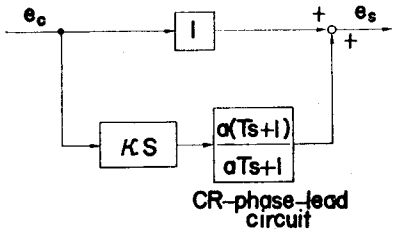

Fig. 5. Configuration of the linear compensation network with a *CR*-phase-lead circuit.

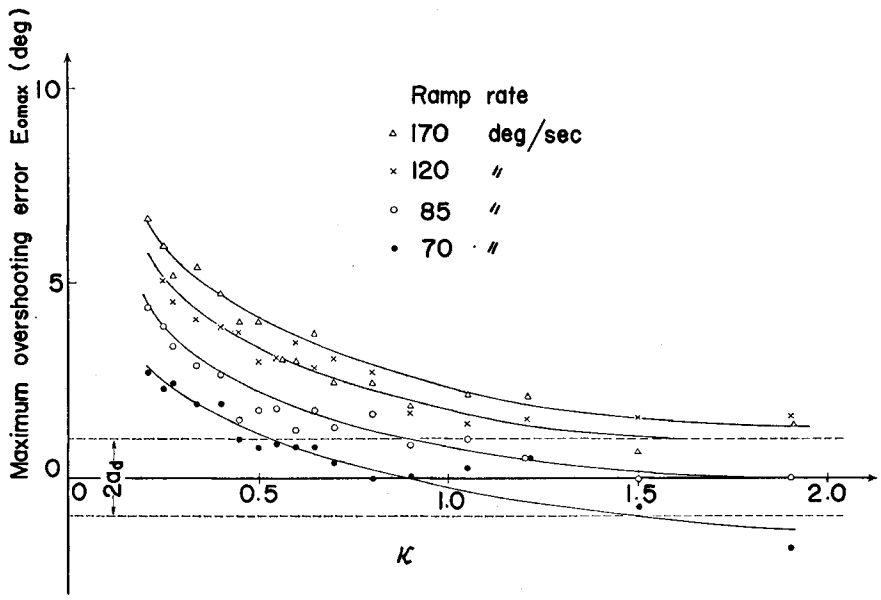

Fig. 6. Experimental plots of $E_{0\max}$ vs κ with the value of the ramp rate as a parameter for the compensation network as shown in Fig. 2.

Although linear compensation techniques presented in this section do give improved performance, the introduction of certain nonlinear elements into a control system can do better by simpler, smaller, and more economical elements for the compensation of inherent nonlinearities[8].

Therefore, in the following section, introdution of a simple nonlinearity will be proposed.

4. Analysis of the Nonlinear Compensation Device

In general, saturation in amplifiers, backlash in gear trains, and a dead zone or coulomb friction in motors are typical inherent nonlinearities which are present a priori in any practical servo systems. An example of intentional nonlinearity if a nonlinearly damped system which optimizes the response under the given condition. The on-off relay servo, which applies full torque as soon as the error exceeds a specified value, is another example of an intentionally nonlinear system[9].

Usually, nonlinearities may be intentionally introduced into control systems for three basic reasons[8]:

1) to make the system simpler, more economical, and smaller;
2) to compensate for inherent nonlinearities;
3) to "optimize" system performance.

The purpose of this section is to introuduce an intentional nonlinear compensation device and to indicate that the compensation technique used in our study meets our requirements, that is, whatever the rate of ramp input, the maximum overshooting error $E_{0\max}$ should be held within a given tolerable value.

4.1. Relation between κ and r

In the previous section the effect of a compensation device consisting of a linear element only was discussed using experimental results of a model and an analog computer. As was pointed out in the discussion, however, a satisfactory result was not obtained.

It is evident from the result that the maximum overshooting error $E_{0\max}$ is a certain function of κ, with a ramp rate as a parameter.

Therefore we define

$$E_{0\max} = \Phi(\kappa; r) \tag{2}$$

where Φ is a function of κ and r is a parameter. It is convenient to assume that Φ is given in the form of a graph or a set of data points rather than an analytically expressed function.

We aim to hold E_0 within a given tolerance regardless of the value of ramp rate.

Now let a given tolerance by δ. Setting $E_{0\max}=\delta$ in Eq. (2), we obtain the relation between κ and r:

$$\kappa = \Psi(r; \delta) \tag{3}$$

where Ψ is a function of r and δ is a parameter. Thus the problem reduces to the determination of the proper nonlinearity such that the equivalent gain κ changes according to the functional relation $\Psi(r; \delta)$.

4.2. Inverse describing function[10]

The problem now may be stated as follows. Given an equivalent gain characteristic, what is a single-valued symmetrical nonlinearity that has this gain?

In general, there are two methods to find the answer. The first is the representation of a nonlinear input-output relationship by a polynomial and the second is a piecewise-linear approximation.

Many physical nonlinearities are best approximated by a polynomial. Let us consider here the general symmetrical single-valued nonlinearity given by two kinds of representation, power series and Fourier sine series.

The general form of the nonlinearity is given by

$$z = f(y) \tag{4}$$

where the output z is a symmetrical single-valued function of the input y. (See Fig. 7)

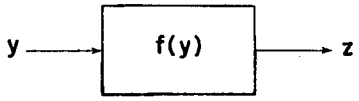

Fig. 7. Symmetrical single-valued nonlinearity $f(y)$.

For symmetrical single-valued nonlinearities there is no phase shift in the functional relation, and thus the equivalent gain $N(M)$ is given by

$$N(M) = \frac{1}{\pi M}\int_0^{2\pi} f(M\sin\theta)\sin\theta\, d\theta \tag{5}$$

where M is the input-signal amplitude.

(a) Development of nonlinear function $f(y)$ in power series

Let the input-output characteristics be $P(y)$, where,

$$f(y) \equiv P(y) = a_1 y + a_3 y^3 + \cdots + a_{2n-1} y^{2n-1}. \tag{6}$$

Substituting Eq. (6) into Eq. (5), we have,

$$N_n(M) = \frac{1}{\pi M}\int_0^{2\pi} a_{2n-1}(M\sin\theta)^{2n-1}\sin\theta\, d\theta \tag{7}$$

where

$$N(M) = \sum_{k=1}^{n} N_k(M). \tag{8}$$

Now we use the following trigonometric function formula

$$\sin^{2k-1}\theta = \frac{1}{2^{2k-2}}\sum_{m=0}^{k-1}(-1)^{m+k-1}\binom{2k-1}{m}\sin\{(2k-2m-1)\theta\}. \tag{9}$$

We have

$$\begin{aligned} N_k(M) &= \frac{1}{\pi M}\sum_{m=0}^{k-1}\frac{(-1)^{m+k-1}}{2^{2k-2}}\binom{2k-1}{m}a_{2k-1}M^{2k-1}\int_0^{2\pi}\sin\{(2k-2m-1)\theta\}\sin\theta\, d\theta \\ &= \frac{1}{\pi M}\sum_{m=0}^{k-1}\frac{(-1)^{m+k-1}}{2^{2k-2}}\binom{2k-1}{m}a_{2k-1}M^{2k-1} \\ &\quad\times\frac{1}{2}\left[\int_0^{2\pi}\cos\{(2k-2m-2)\theta\}\,d\theta - \int_0^{2\pi}\cos\{(2k-2m)\theta\}\,d\theta\right] \\ &= \frac{1}{2^{2k-2}}\binom{2k-1}{k-1}a_{2k-1}M^{2k-2}. \end{aligned}$$

Thus

$$N(M) = \sum_{k=1}^{n}\frac{1}{2^{2k-2}}\binom{2k-1}{k-1}M^{2k-2}a_{2k-1}. \tag{10}$$

Given $M_i$and $N(M_i)$, where $i=1, 2, 3, \cdots, n$, Eq. (10) can be considered as an $n\times n$ linear simultaneous equation with regard to a_{2k-1} and the coefficients of the series $P(y)$ may be determined.

(b) Development of nonlinear function $f(y)$ in Fourier sine series

Now let us approximate the input-output characteristic by Fourier sine series, $S(y)$, where,

$$f(y) \equiv S(y) = b_1 \sin y + b_2 \sin 2y + \cdots + b_n \sin ny \,. \tag{11}$$

Substituting Eq. (11) into Eq. (5), we have,

$$N_n(M) = \frac{1}{\pi M}\int_0^{2\pi} b_n \sin (nM \sin\theta) \sin\theta \, d\theta \tag{12}$$

where

$$N(M) = \sum_{k=1}^{n} N_k(M) \,. \tag{13}$$

Here we utilized the following formula

$$\sin (\beta \sin\theta) = 2\sum_{m=0}^{\infty} J_{2m+1}(\beta) \sin\{(2m+1)\theta\} \tag{14}$$

where

$$J_r(\beta) = \sum_{l=0}^{\infty} \frac{(-1)^l}{l!(l+r)!}\left(\frac{\beta}{2}\right)^{2l+r} \tag{15}$$

(the Bessel function of order r).

We then obtain the following relation.

$$\begin{aligned} N_k(M) &= \frac{2b_k}{\pi M}\int_0^{2\pi} \sum_{m=0}^{\infty} J_{2m+1}(kM) \sin\{(2m+1)\theta\} \sin\theta \, d\theta \\ &= \frac{b_k}{\pi M}\sum_{m=0}^{\infty} J_{2m+1}(kM)\left[\int_0^{2\pi} \cos(2m\theta)\, d\theta - \int_0^{2\pi} \cos\{(2m+1)\theta\}\, d\theta\right] \\ &= \frac{2b_k}{M} J_1(kM) \,. \end{aligned}$$

Thus

$$N(M) = \sum_{k=1}^{n}\sum_{l=1}^{\infty} \frac{(-1)^l k^{2l-1} b_k}{l!(l-1)!}\left(\frac{M}{2}\right)^{2l-2} \,. \tag{16}$$

Given M_i and $N(M_i)$, where $i=1, 2, 3, \cdots, n$, Eq. (16) can be considered as an $n\times n$ linear simultaneous equation with regard to b_k. Solving this equation, the coefficients of the series $S(y)$ may be determined.

In these procedures, we have the following three steps:

Step (I) Obtain the relation $E_{0\max}=\Phi(\kappa; r)$ (graphically)

Step (II) Obtain the relation $\kappa=\Psi(r;\delta)$ (graphically)

Step (III) Given Eq. (10) or Eq. (16), solve these equations using Step (II) and determine the input-output characteristics.

4.3. Examples

Before finding out the desirable nonlinearity, let us consider in somewhat more detail a polynomial approximation of given equivalent gain plots.

Consider two symmetrical, single-valued nonlinearities, saturation and dead zone, shown in Figs. 8 and 9 respectively. Assume that the equivalent gain of the nonlinearity is given as plotted in Fig. 10.

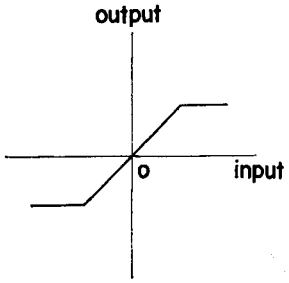

Fig. 8. Nonlinear characteristic of saturation.

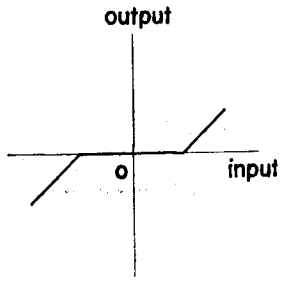

Fig. 9. Nonlinear characteristic of dead zone.

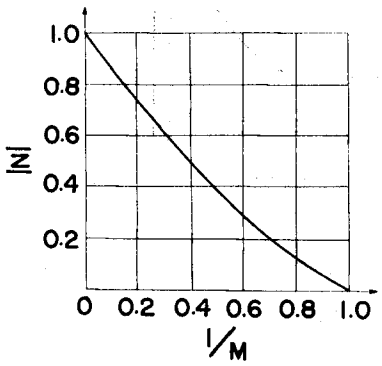

Fig. 10. Normalized describing function for saturation.

Now we find the expression for the nonlinearity. Using a digital computer, we solve Eq. (10) or Eq. (16) for any given M and n. The experimental results are shown in Fig. 11 and Fig. 12. The former is the representation of the first nonlinearity by a power series and the latter by a Fourier sine series.

The results exactly meet our expectations: the first has been recognized as

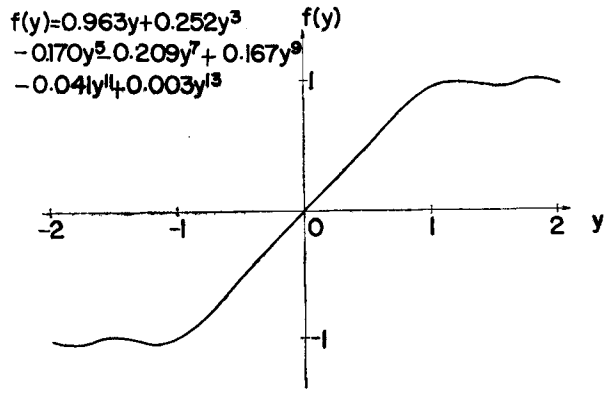

Fig. 11. Graph of $f(y)$.

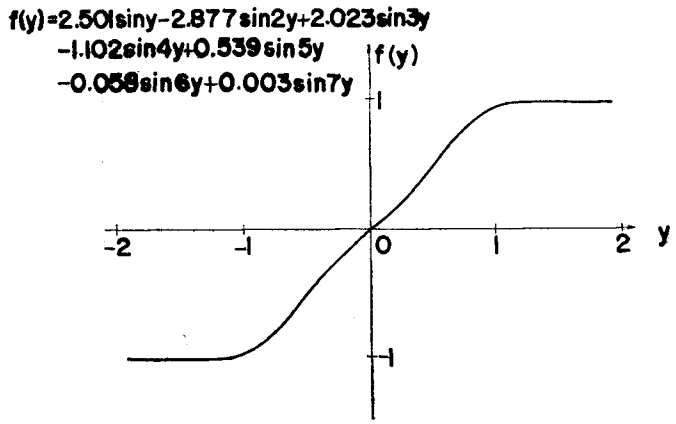

Fig. 12. Graph of $f(y)$.

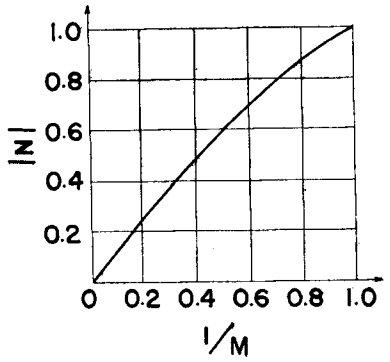

Fig. 13. Normalized describing function for a dead zone.

saturation. Similarly, the second nonlinearity, the equivalent gain curve of which is shown in Fig. 13, can be obtained and recognized as the dead zone, as shown in Fig. 14 and 15.

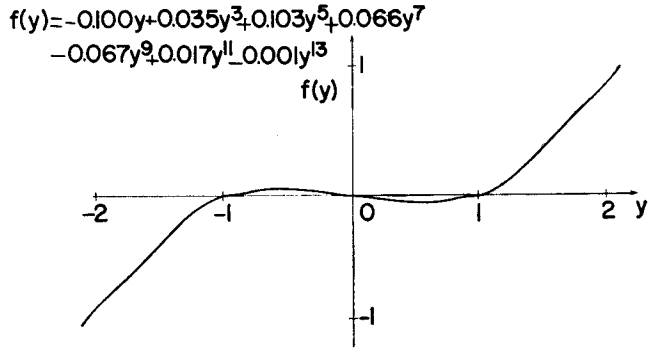

Fig. 14. Graph of $f(y)$.

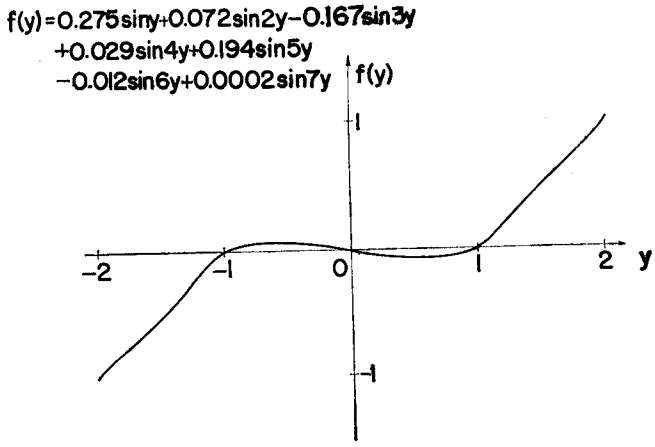

Fig. 15. Graph of $f(y)$.

From these examples, we can see that the two nonlinearities can be practically approximated by a polynomial. We have here two problems. Firstly, what is the appropriate number of terms that should give satisfactory approximation? We must make use of a digital computer to answer this and determine experimentally the desirable number of terms. Secondly, we do not know which data to choose. This problem must also be solved by means of a digital computer. In practice we vary the number of terms n from 5 to 12 and selcet just as many data as the number of terms.

By the calculation using the digital computer, we found that for $n=7$, a good representation can be realized)both by a power series and a Fourier sine series. Comparing these two representations, we see that for the same number of terms, the latter gives better results than the former. This appears to be due to the weighting effect of the error of the approximation.

4.4. Application

We will now show that the output of the derivative element κs is in proportion to the ramp rate. As the input to the system is a ramp input, its response is as illustrated in Fig. 16 (a). This is easily verified by analog computer. E_0 is the transient error, or the overshooting error previously defined. The input to the derivative element κs is the steady-state error e_c and the shape is as shown in Fig. 16 (b). Hence, the output of the derivative element can be approximated by a pulse whose magnitude is in proportion to the ramp rate. Fig. 16 (c) illustrates this fact.

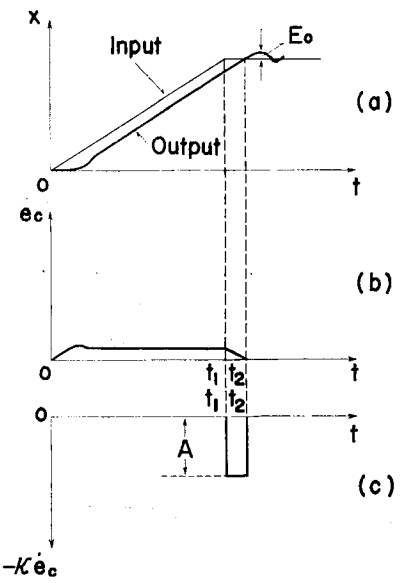

Fig. 16. Typical transient response of servo-systems following a ramp input.
(a) Relation between input and output.
(b) Error.
(c) Error rate.

Taking account of this, we now employ the inverse describing function method for the determination of the nonlinearity that should satisfy our requirements.

Step (I)

$\Phi(\kappa; r)$ is given in the form of a set of data points shown in Fig. 6, where $E_{0\max}$ is in degrees, and the parameter is the ramp rate in degrees per second.

Step (II)

In order to obtain the relationship $\Psi(r; \delta)$, put $\delta=2°$ or $\delta=3°$, where δ is in terms of the angular difference of the two synchros. Then, from Fig. 6, $\Phi(r; \delta)$ is obtained as shown in Fig. 17.

Step (III)

As mentioned before, r corresponds to M and κ to $N(M)$. Substituting these values into Eq. (10) or Eq. (16), the input-output characteristics can be obtained.

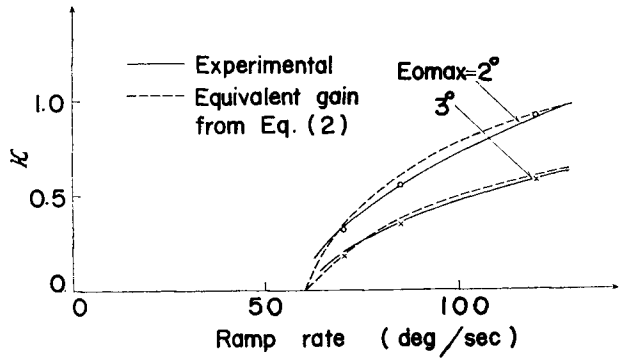

Fig. 17. Relation between κ and ramp rate with $E_{0\max}$ as a parameter.

Here note that the n equations should determine the n a_{2n-1}'s or b_n's.

We now choose $n=7$ and $l=8$ using the results obtained from examples in the previous section. Solving Eq. (10) and Eq. (16), the coefficients are determined, and then the desirable nonlinearity is obtained as follows:

$$f(y) = -0.131y-0.008y^3+0.096y^5+0.106y^7-0.040y^9+0.001y^{11}+0.0004y^{13},$$

or

$$f(y) = 2.001 \sin y-1.801 \sin 2y+0.716 \sin 3y-0.307 \sin 4y+0.150 \sin 5y \\ -0.016 \sin 6y+0.001 \sin 7y.$$

Fig. 18 and Fig. 19 illustrate these results. As we have expected, the functions $f(y)$ have the input-output characteristics similar to those for a dead zone. It is therefore reasonable to introduce a dead zone following the derivative element κs.

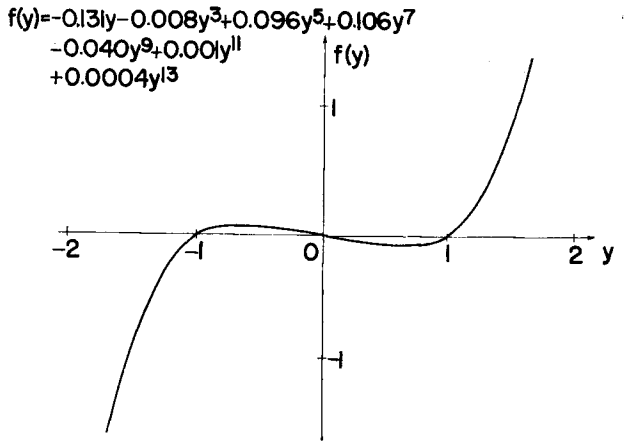

Fig. 18 (a)

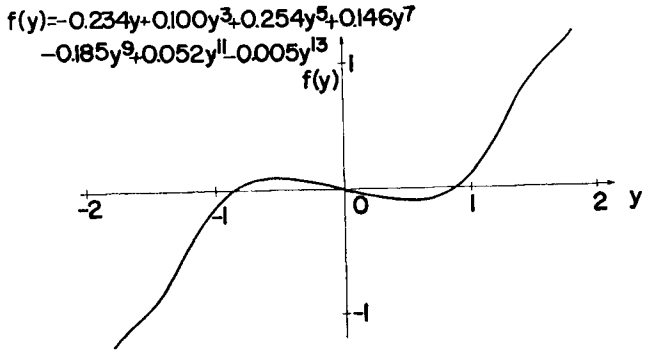

(b)

Fig. 18. Graph of $f(y)$.

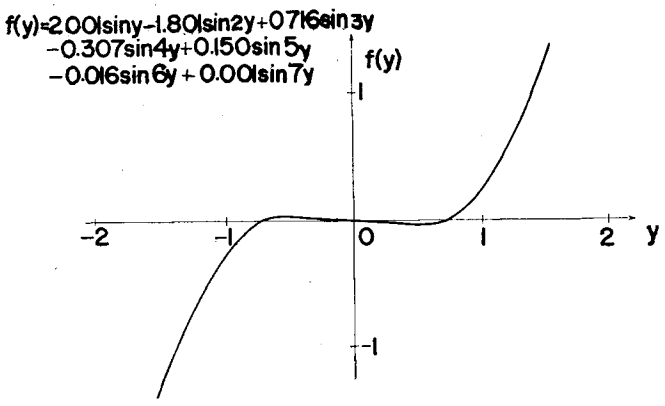

(a)

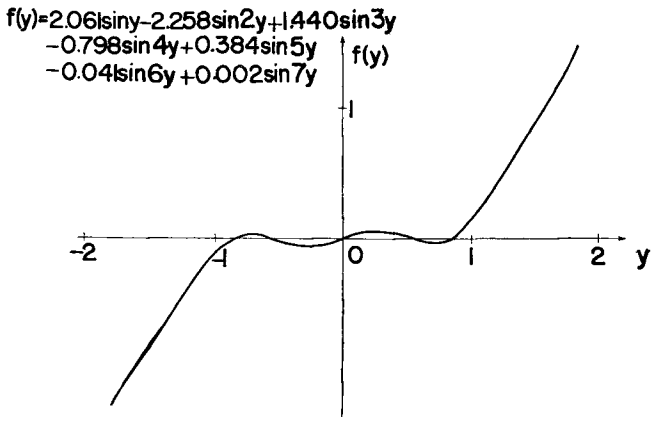

(b)

Fig. 19. Graph of $f(y)$.

Such a nonlinear compensation is illustrated in Fig. 20.

Satisfactory results are in fact obtained from experiments using a model in which the nonlinear compensation with a dead zone is inserted in this way. The results are shown in Fig. 21 and this serves our primary purpose.

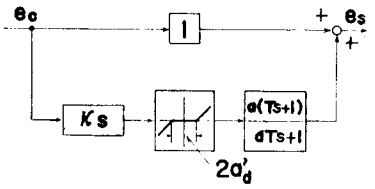

Fig. 20. Nonlinear compensation network with dead zone.

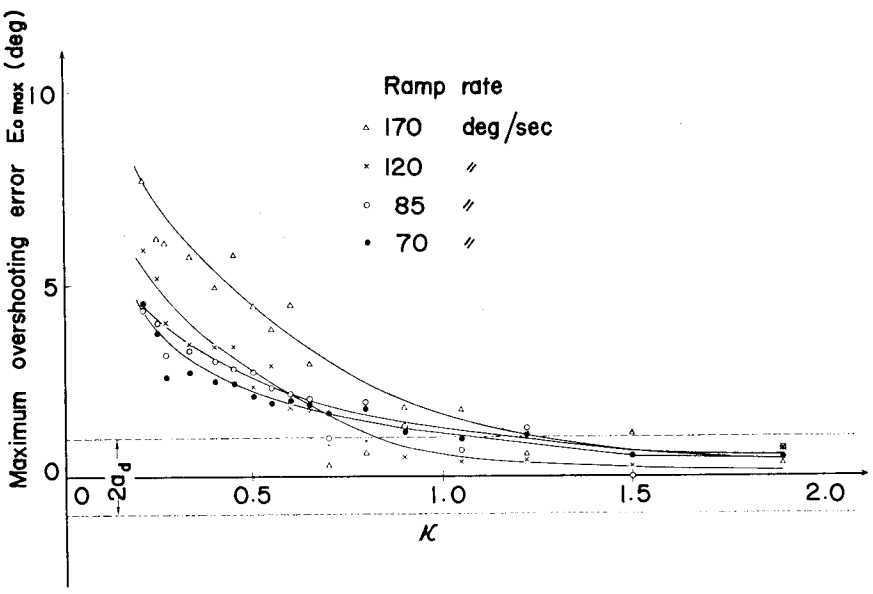

Figs. 21. Experimental plots of $E_{0\max}$ vs κ with the value of the ramp rate as a parameter for the compensation network as shown in Fig. 20.

5. Stability Analysis

There are a number of methods available to check the stability of systems with a nonlinear element. For the systems with more than one nonlinear element, however, the analysis is rather complex[11]. Only some specific cases have been treated in any detail so far. In the system of Fig. 1, we have the three typical nonlinear elements. We shall treat this system by the linearization and the describing function technique and investigate the stability as well as the influence of these nonlinearities on the performance of the system.

5.1. Method of analysis

In order to investigate the stability of the system, the input is set to zero. The

dead zone inherent to pre-amplifier may then be transferred to the position following that of the backlash of the gear. Namely, these two elements are put together and the describing function of the combined element, $N(\theta)$, is obtained where θ is the amplitude of input to the backlash element. There is another nonlinear element, the saturation, in the magnetic amplifier circuit in the minor loop. The describing function of the saturation element depends only on the input amplitude and is independent of the phase. In view of this fact, the saturation element is first replaced by a constant gain α and the stability limit is obtained for this system as shown in Fig. 22. Then, the describing function will be introduced and the stability of the original system discussed.

Now the block diatram of Fig. 1 may be simplified to the one shown in Fig. 23. Here $G(s)$ and $G_c(s)$ are given by

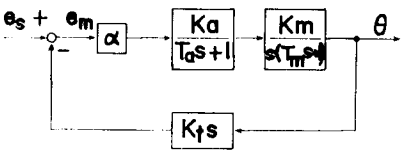

Fig. 22. Substitution of a linear element with simple gain α for the saturation characteristic element.

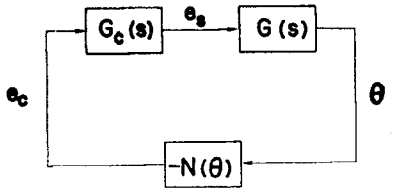

Fig. 23. Block diagram of the system of Fig. 1 for stability analysis.

$$G(s) = \frac{\alpha K_a K_m}{s\{T_a T_m s^2 + (T_a + T_m)s + \alpha K_a K_m K_t + 1\}} \tag{17}$$

$$G_c(s) = \frac{aT\kappa s^2 + a(T+\kappa)s + 1}{aTs + 1} . \tag{18}$$

The characteristic equation of the simplified system of Fig. 23 is given by

$$1 + G_c(j\omega)G(j\omega)N(\theta) = 0 . \tag{19}$$

Putting

$$G_c(j\omega)G(j\omega) = G_L(j\omega) , \tag{20}$$

we have

$$G_L(j\omega) = -\frac{1}{N(\theta)} . \tag{21}$$

Drawing the vector locus $G_L(j\omega)$ and the amplitude locus $N^{-1}(\theta)$ on the gain phase plane and by seeing whether these two loci intersect each other, we can investigate the stability of the system of Fig. 1.

5.2. Gain-phase diagram

There are two parameters α and κ in the characteristic equation, Eq. (6). Fig. 24 shows the group of curves in which κ is kept constant and α is varied as

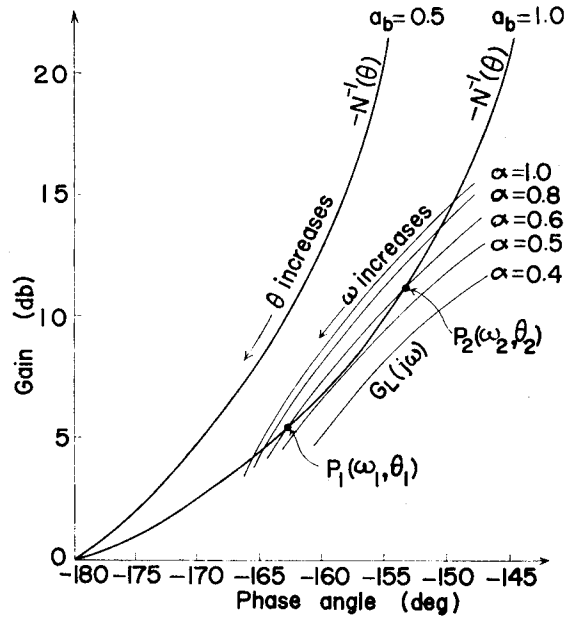

Fig. 24. Gain-phase diagram for the calculation of critical gain curve for $\kappa=0.5$.

the parameter. The values of the various other constants are chosen as follows.

$$a=0.36,\quad T=0.022,\quad a_d=1.0,\quad a_s=5.0,\quad K_a=100.0,\quad K_m=60.0,$$
$$K_t=8.35\times10^{-5},\quad T_a=0.25,\quad T_m=0.5$$

The amplitude loci drawn are for the cases of $2a_b=1$ and 2. In Fig. 24, the two intersections of the vector locus and the amplitude locus are denoted by P_1 and P_2. P_1 represents a stable limit cycle with ω_1 and θ_1, while P_2 represents and unstable oscillation with ω_2 and θ_2. It is found that the system is stable either for $\theta>\theta_1$ or for $\theta<\theta_2$ whereas it is unstable for $\theta_2<\theta<\theta_1$, where θ is the input to the nonlinear element $N(\theta)$.

It is clear from Fig. 24 that for large α the two loci have intersections. This is well anticipated and this means that for a large loop gain of the system it is unstable.

Now if we draw a gain-phase diagram as in Fig. 25 and superpose the constant κ curve on it, then we can see how the system is stabilized by increasing κ.

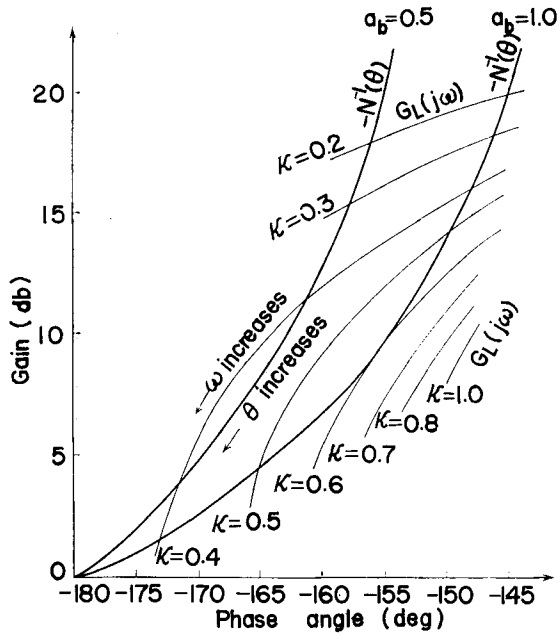

Fig. 25. Stability analysis with respect to the values of κ by using gain-phase diagram ($\alpha=1$).

5.3. Critical gain curve ($\alpha-e_m$ diagram)[10]

It is convenient to use a critidcal gain curve explained in the following to give an overall picture of the system stability. Here, κ will be taken as the parameter and the relation between α and e_m will be found. The resulting figure may be called $\alpha-e_m$ curves.

If we draw gain-phase diagram of Fig. 24 with parameter α, for various values of κ, we obtain two intersections P_1 and P_2 for each value of α. We now seek the relation between α and e_m, calculating the input amplitude e_m by the following equation.

$$e_m = \left|\theta \cdot \left[\frac{(T_a s+1)(T_m s+1)s}{K_a K_m \alpha}\right]_{s=j\omega}\right|. \tag{22}$$

Drawing this relation in $\alpha-e_m$ curves, we have one curve for a value of κ. For example, the critical gain curve for $\kappa=0.5$ is as shown in Fig. 26.

Any intersection in the range to the right of the minimum point (or maximum point in Fig. 27) on the critical curve (shown by full line) with the describing function curve, will represent a stable limit cycle. On the other hand, any intersection on the left side of the minimum point on the critical curve (shown by dotted line) will represent an unstable limit cycle. For a given α, then, the portion

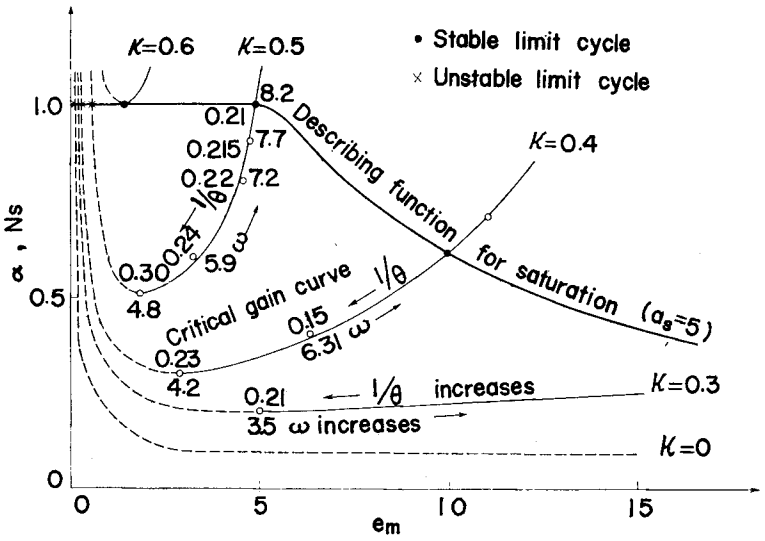

Fig. 26. Critical value of α vs e_m with κ as a parameter and describing function for saturation.

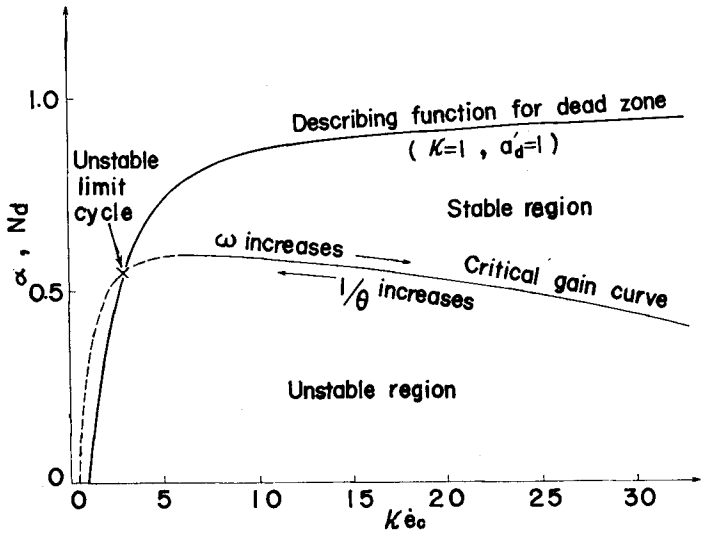

Fig. 27. Critical value of α' vs e_c and describing function for dead zone following κs.

within the critical gain curve will represent the region of instability, corresponding to the portion between P_2 and P_1 in Fig. 24.

Now, in order to see the stability of the original system with saturation, the describing function will be superposed on the $\alpha - e_m$ curve. If the critical gain

curve corresponding to a value of κ intersects the describing function curve, the point of intersection on the left represents an unstable limit cycle, whereas the point on the right represents a stable limit cycle. If there is no intersection, then the system is stable.

Inspecting Fig. 26, we see that the system is stable for larger values of κ than 0.6. A similar procedure yields the result that κ should be larger than 0.445 for the system with $a_b=0.5$.

As to the effect of backlash on stability, it is found that κ may be taken smaller for a smaller backlash and should be taken larger for a larger backlash to assure stability.

It is to be noted that the gain is unity at the point where the critical gain curve and the curve for describing fucntion touches each other. Therefore, as far as the stability is concerned, the saturation element may be considered as a simple linear element with gain unity.

Now, we replace the dead zone element by a simple gain α', and using the relation between input amplitude $\kappa\dot{e}_c$, we obtain the critical gain curve as shown in Fig. 27. If we superpose the describing function of the dead zone, it intersects the critical gain curve in the unstable region. Calculation shows that for the width of the backlash $2a_b=1$, the width of dead zone a_d' must be kept below 0.5, and for $2a_b=2$, a_d' must be less than 0.3.

6. Conclusion

A method is presented to determine a desirable nonlinearity to be introduced into the system in comparatively simple steps, using experimental results of a model and the inverse describing function.

By using nonlinear compensation network, overshooting error of a two-dimensional contouring servomechanism tracing a corner of a prescribed figure was held within an allowable limit. The application of the result of analysis to an automatic flame cutting machine gave satisfactory performance.

With respect to this example, a method is presented of analyzing systems with two or more nonlinearities for stability and for the influence on it of the character of nonlinear elements.

Future problems will be to obtain analytically the transient response of nonlinear systems and to apply the result to the synthesis.

Acknowledgement

Our thanks are due to Profs. Tokumaru, Sunahara and Fukawa of Kyoto

University for their significant discussions, to Mr. Terao, Tsutsumi and Yamane of Ishikawajima-Harima Heavy Industry for their help in applying the analysis to the automatic flame cutting machine and to Mr. Hiraoka, Nagai and Yonetani, Kyoto Univ., for their assistance in numerical calculations.

References

1) V.A. Taran; Automation and Remote Control, Vol. 25, No. 1, pp. 128–137, January (1964).
2) C.N. Shen; Trans. ASME, Vol. 78, No. 3, pp. 585–592, April (1956).
3) C.N. Shen; Proc. the First IFAC Congress, Moscow (1960).
4) A.K. Mahalanabis; Trans. AIEE, Vol. 80, Part II, pp. 277–284, November (1961).
5) C.N. Shen and H. Wang; Trans. IEEE, Vol. 71, pp. 128–135, March (1964).
6) F.J. Ellert; Trans. AIEE, Vol. 74, Part II, pp. 345–354, January (1956).
7) H.E. Vigour; Trans. IEEE, No. 60, pp. 120–124, May (1963).
8) T.M. Stout; Control Engineering, Vol. 3, No. 4, April (1956).
9) S.M. Shinners; Control System Design, John Wiley & Sons Inc., (1964).
10) J.E. Gibson; Nonlinear Automatic Control, McGraw-Hill Book Co., (1963).
11) E.A. Freeman; Proc. IEE, Part C, pp. 665–675, July (1962).